

GAN-based defect transfer model for steel surface defects generation

Student: Francesco Gazzola
Supervisor: Emanuele Menegatti, Stefano Totaro
Co-supervisor: Alberto Bacchin

Padova, 27-11-2023

DEPARTMENT OF
INFORMATION
ENGINEERING

UNIVERSITY OF PADOVA

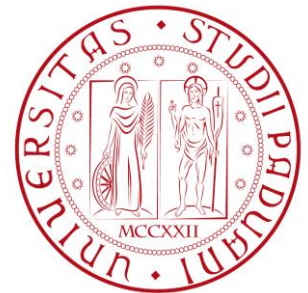
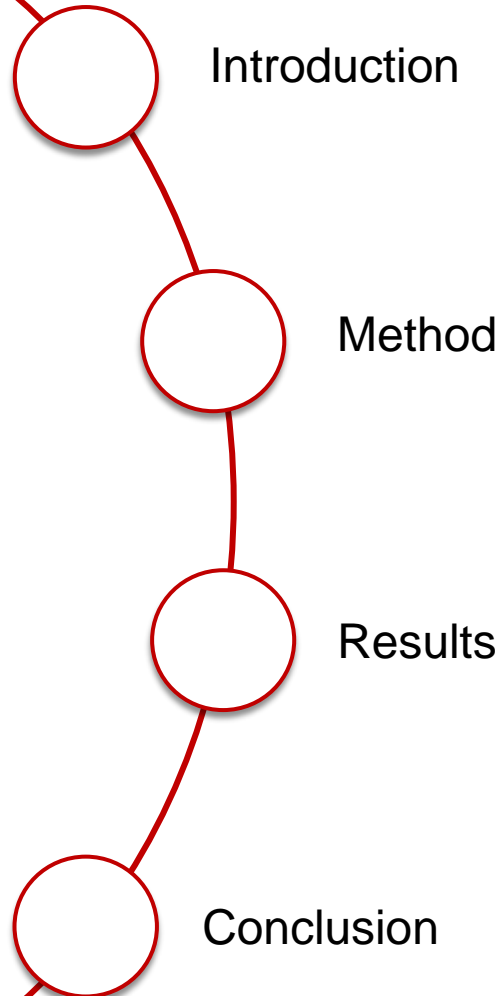
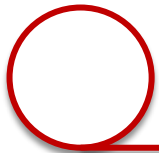


Table of contents

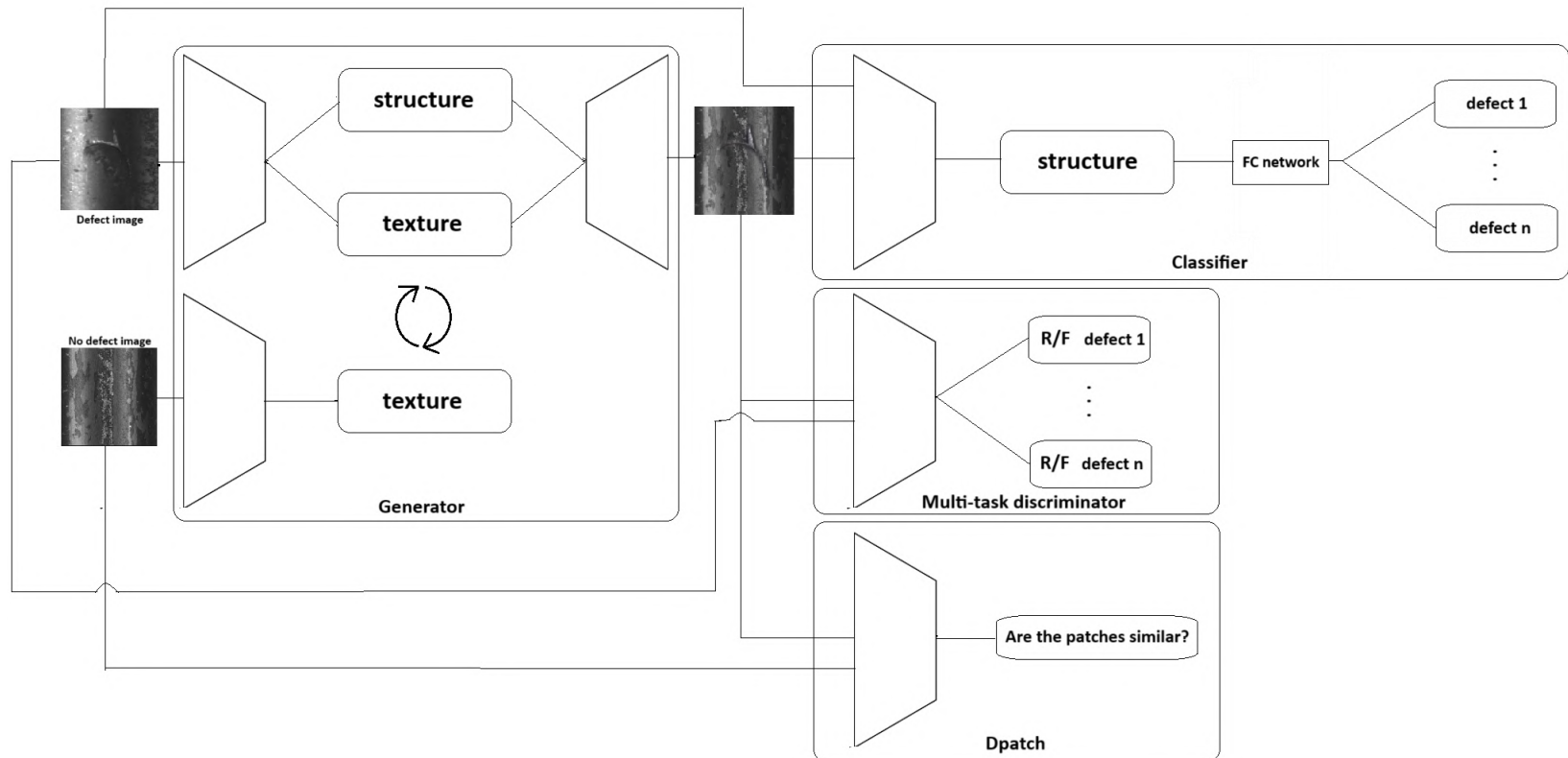




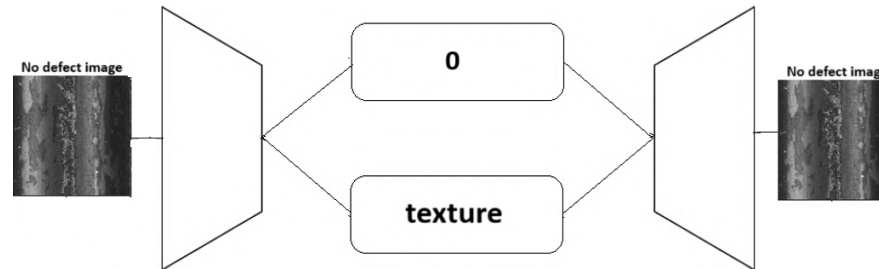
- During the steel manufacturing process, diverse defects might occur due to the different processing techniques such as the rolling equipment
- Defects can lead to safety hazard and reduce the product performance and quality
 - we need to detect the defects
 - But little data in a real-world scenario: it is easy to collect no-defective images, but defects images are very few. This leads to bad accuracy of a classifier.
 - we need data-augmentation

THESIS OBJECTIVE: given images of defects on materials of texture X , transfer them to images of surfaces with a different texture Y in order to enhance diversity

- Based on the swapping autoencoder
 - Disentangled learning



- Anchor domain hypothesis



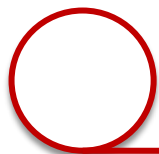
- Given an image X_i s.t. $(z_s^i, z_t^i) = \text{Encoder}(X_i)$ are the structure and the texture code, and $X_1 = \text{defective image}$, $X_2 = \text{no-defective image}$, $X_3 = G(z_s^1, z_t^2)$ i.e. the hybrid image, $X_4 = G(0, z_t^2)$ i.e. the reconstruction of X_2

- Feature reconstruction loss**

$$L_{\text{feature}}(E, G) = \text{MSE}(z_s^3, z_s^1) + \text{MSE}(z_t^3, z_t^2) + \text{MSE}(z_t^4, z_t^2)$$

- Structure consistency loss**

$$L_{\text{Structure}}(E, G) = E_{x \sim X} [|| (x_1 - G(0, z_t^1)) - (G(z_s^1, z_t^2) - x_2) ||_1] \\ + E_{x \sim X} [|| (G(z_s^1, z_t^1) - G(0, z_t^1)) - (G(z_s^1, z_t^2) - x_2) ||_1]$$



- Dataset statistics

scratch	shell	mark	scoring	tear	notching	normal
105	28	163	25	167	40	7262

Table 4.1: Original industrial set

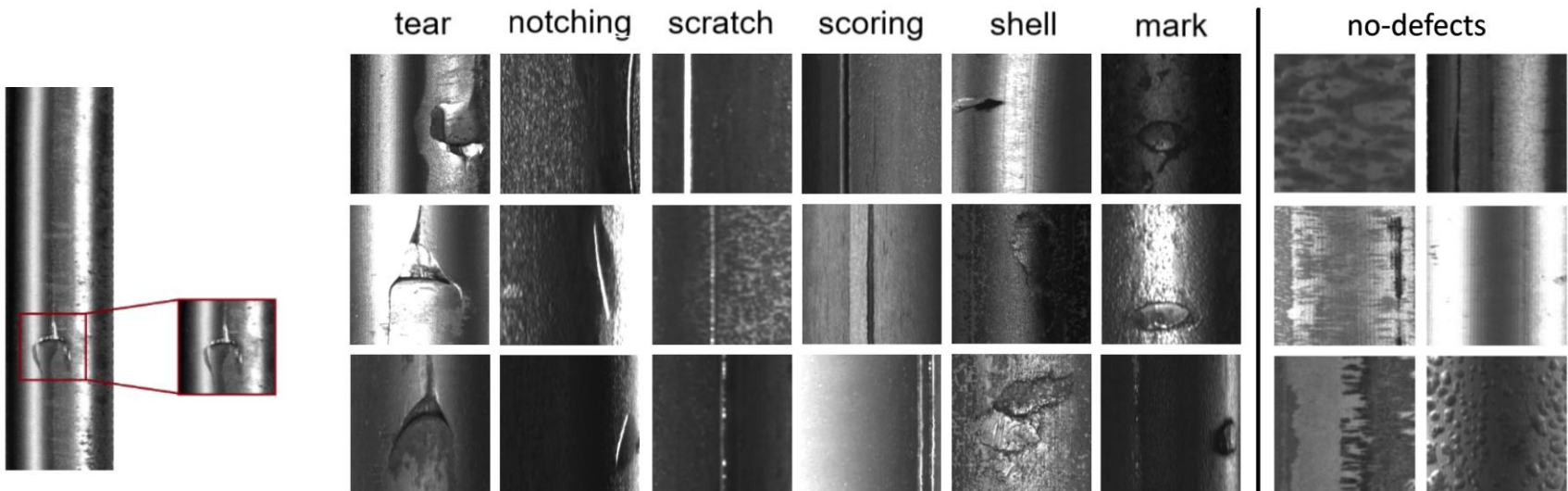


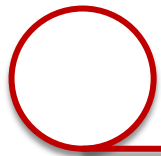
+ horizontal and vertical flip

scratch	shell	mark	scoring	tear	notching	normal
105	84	163	75	167	120	727

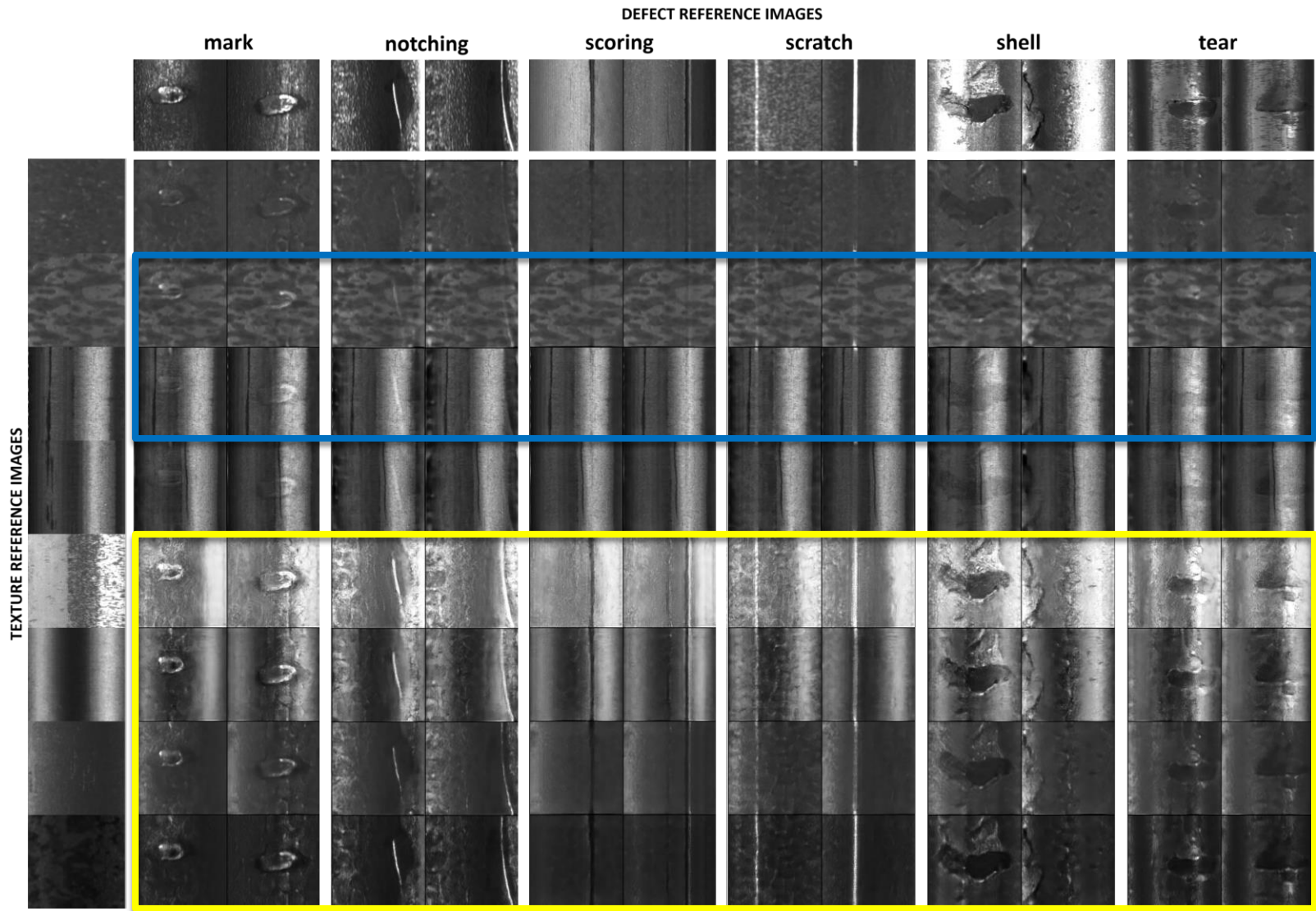
Table 4.2: Training set

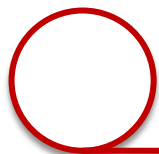
- Training dataset samples example:





Results – Qualitative research

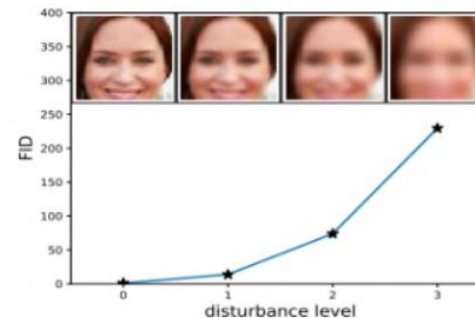
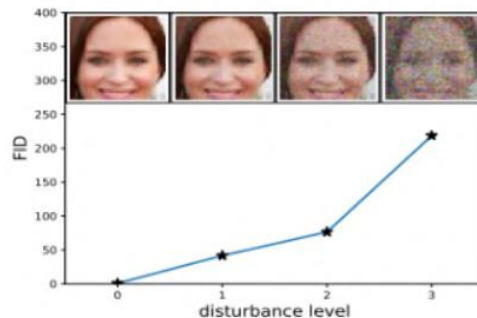




- Fréchet Inception Distance (FID) and Kernel Inception distance (KID) score
 - They are based on statistics: mean and covariance
 - The lower, the better the realness and the diversity of the generated images

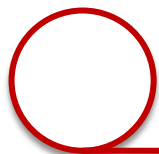
$$FID = ||\mu_r - \mu_g||^2 + Tr(\Sigma_r + \Sigma_g - 2(\Sigma_r \Sigma_g)^{1/2})$$

$$KID = ||\mu_r - \mu_g||^2$$



	scratch	shell	mark	scoring	tear	notching
FID	2.45	4.93	0.72	7.12	0.74	1.15
KID	0.10	0.07	0.13	0.11	0.06	0.19

Table 4.3: Quantitative evaluation



Results – data augmentation

Dataset

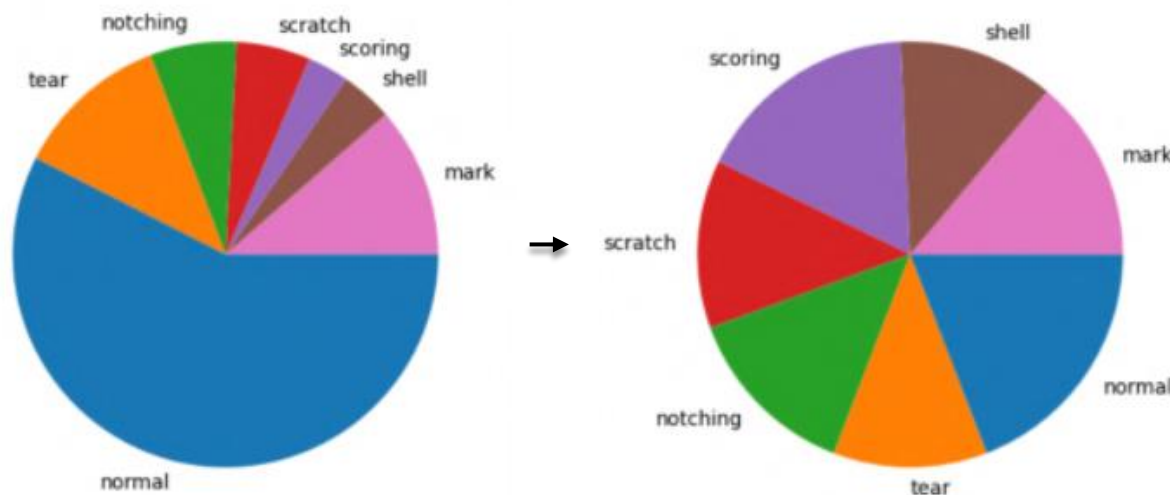
scratch	shell	mark	scoring	tear	notching	normal
59	42	120	33	124	69	604

Table 4.4: Training set for the classifier



scratch	shell	mark	scoring	tear	notching	normal
403	374	438	541	370	428	604

Table 4.7: Augmented training set for the classifier



- Better generalization on the **validation set**

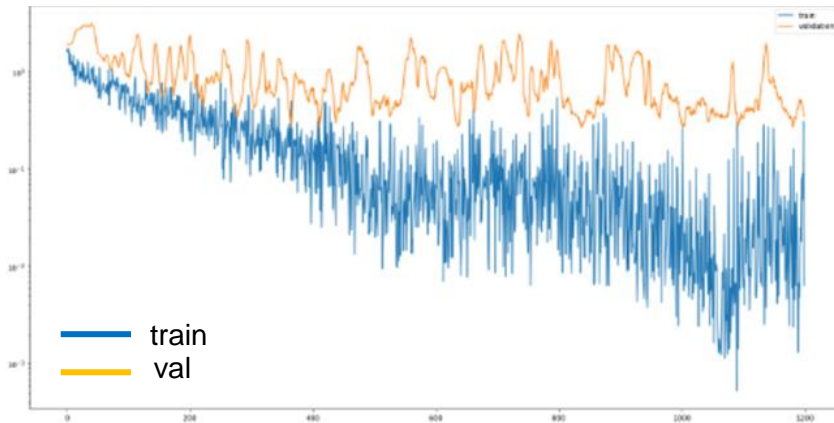


Figure 4.19: Loss ResNet50 classifier on no augmented data

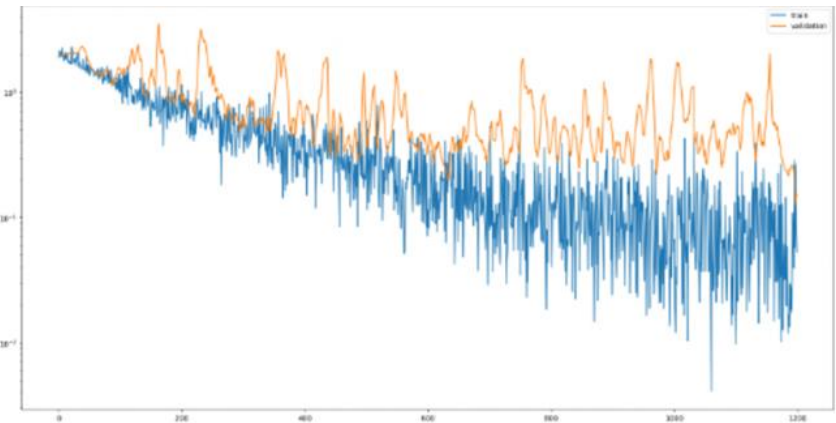


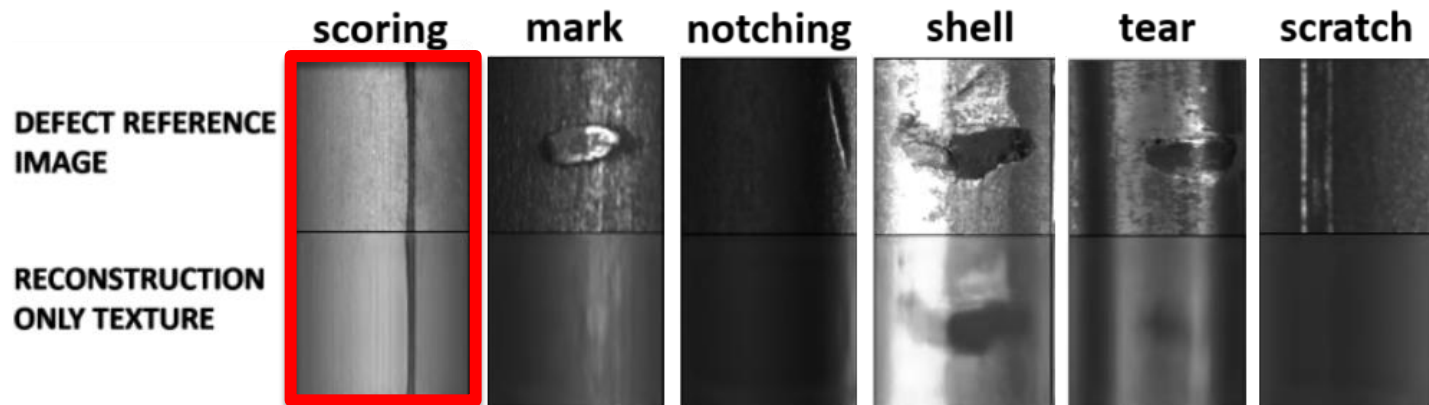
Figure 4.20: Loss ResNet50 classifier on augmented data

- Overall error rate diminished from 9.03% to 5.42% on the **test set**
- Single error rate per class improved too, but the scratch

	scratch	shell	mark	scoring	tear	notching	normal
No augmented	0%	77.8%	6.2%	11.1%	15.2%	0%	0%
Augmented	11.4%	11.1%	3.1%	0.0%	9.1%	0%	0%

Conclusion

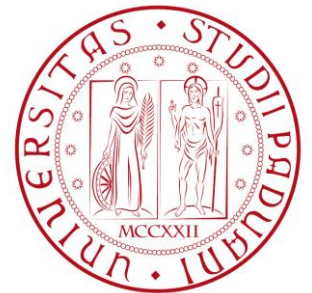
- Transferring the defects across multiple background or changing its style enhances the diversity of the dataset and thus counteracts the data-insufficiency problem in the real-world scenario
- Disentanglement mechanism needs to be improved



Thanks for your attention

DEPARTMENT OF
INFORMATION
ENGINEERING

UNIVERSITY OF PADOVA



- Adversarial loss

$$L_{adv}^D(E, G, D) = E_{x_1, x_2 \sim X} [\log(D(x))] + E_{x_1, x_2 \sim X} [\log(1 - D(G(z_s, z_t)))]$$

- Texture adversarial loss

$$\begin{aligned} L_{CoccurGAN}^D(E, G, D) = & E_{x_2 \sim X} [\log(D_{patch}(crop(x_2), crops(x_2)))] \\ & + E_{x_1, x_2 \sim X} [\log(1 - D_{patch}(crop(G(z_s, z_t)), crops(x_2)))] \end{aligned}$$

- DISCRIMINATORS OBJECTIVE

$$L_D = L_{adv}^D + L_{CoccurGAN}^D$$

○ CLASSIFIER OBJECTIVE

$$L_C = \text{CrossEntropy}(P(y|X), y)$$

○ GENERATOR OBJECTIVE

$$L_G = L_{rec} + 0.5L_{adv}^G + L_{CoocurGAN}^G + L_{Structure} + L_{feature} + L_{cls}^G$$

$$L_{cls}^G(E, G) = \text{CrossEntropy}(P(y|X_{fake}), y)$$

Classification loss

$$L_{CoocurGAN}^G(E, G) = E_{x_1, x_2 \sim X} [-\log(D_{patch}(crop(G(z_s, z_t)), crops(x_2)))]$$

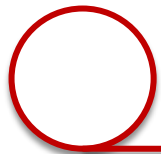
Texture adversarial loss

$$L_{adv}^G(E, G) = E_{x_1, x_2 \sim X} [-\log(D(G(z_s, z_t)))]$$

Non-saturating adversarial loss

$$L_{rec}(E, G) = E_{x \sim X} [\|x_1 - G(z_s^1, z_t^1)\|_1] + E_{x \sim X} [\|x_2 - G(0, z_t^2)\|_1]$$

Image reconstruction loss



Issue – mode collapse

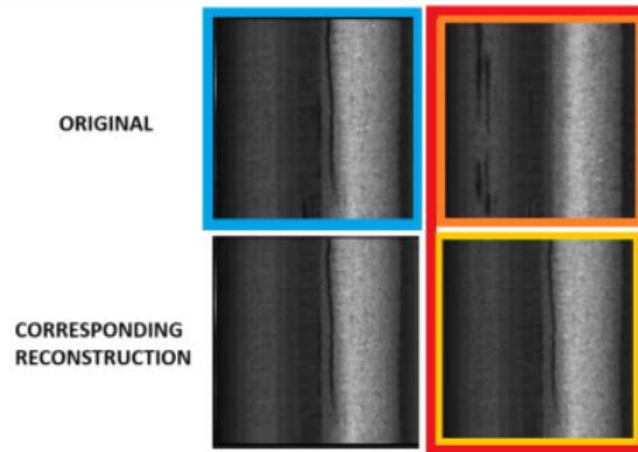


Figure 4.4: Highlighted in red is the suspected case of mode collapse. Given the texture reference image in the the orange box, the model reconstructs it as shown in the yellow box. However its reconstruction is identical to another texture image in the training dataset (shown in the blue box).

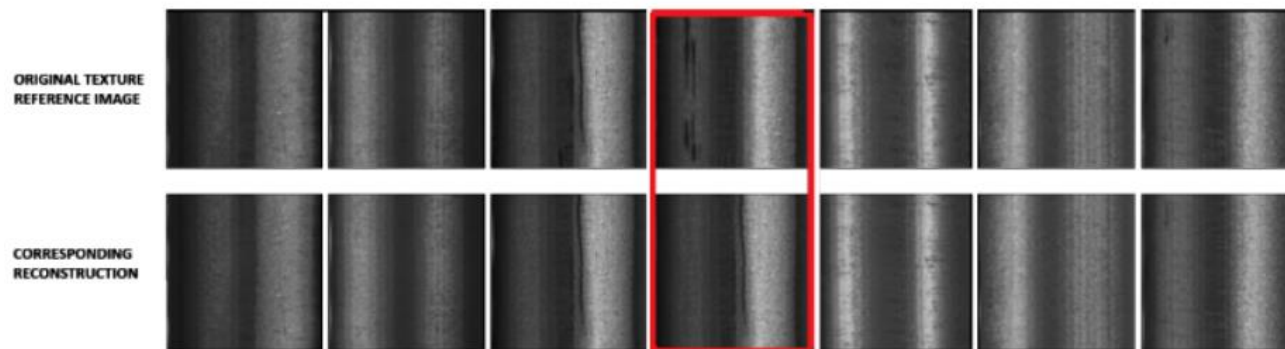
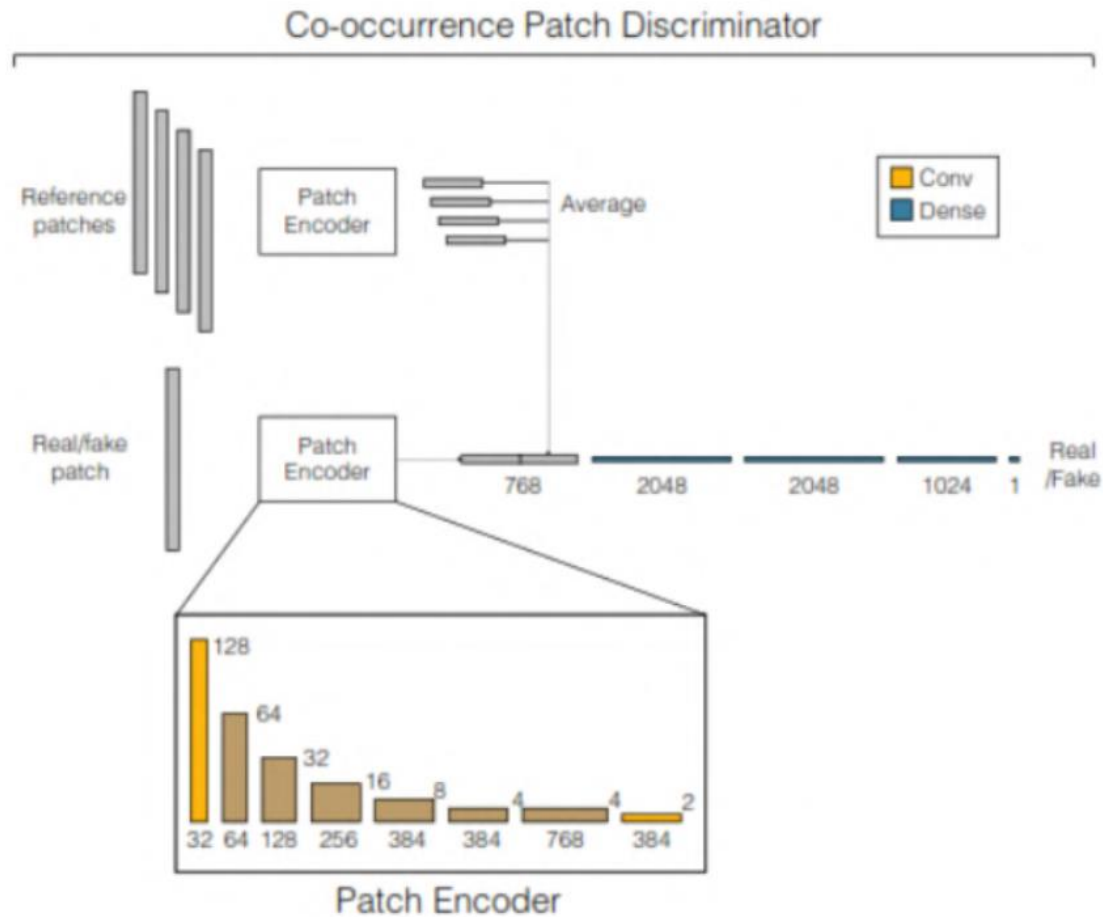


Figure 4.5: Mode collapse study. The first row reports the original image, while the second row represents the corresponding generated image. We can see that although all the images share the same style and texture, only the image at the top in the red box is reconstructed wrongly.

Patch discriminator



Encoder and generator

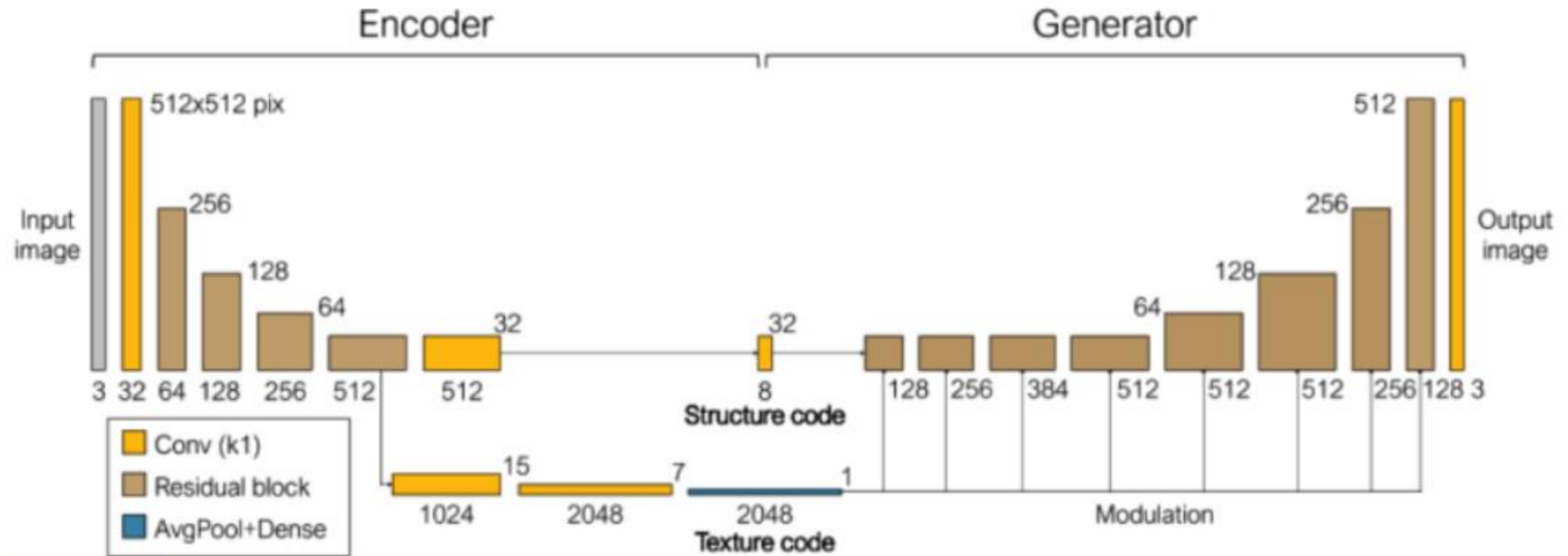


Figure 3.2: Encoder and generator

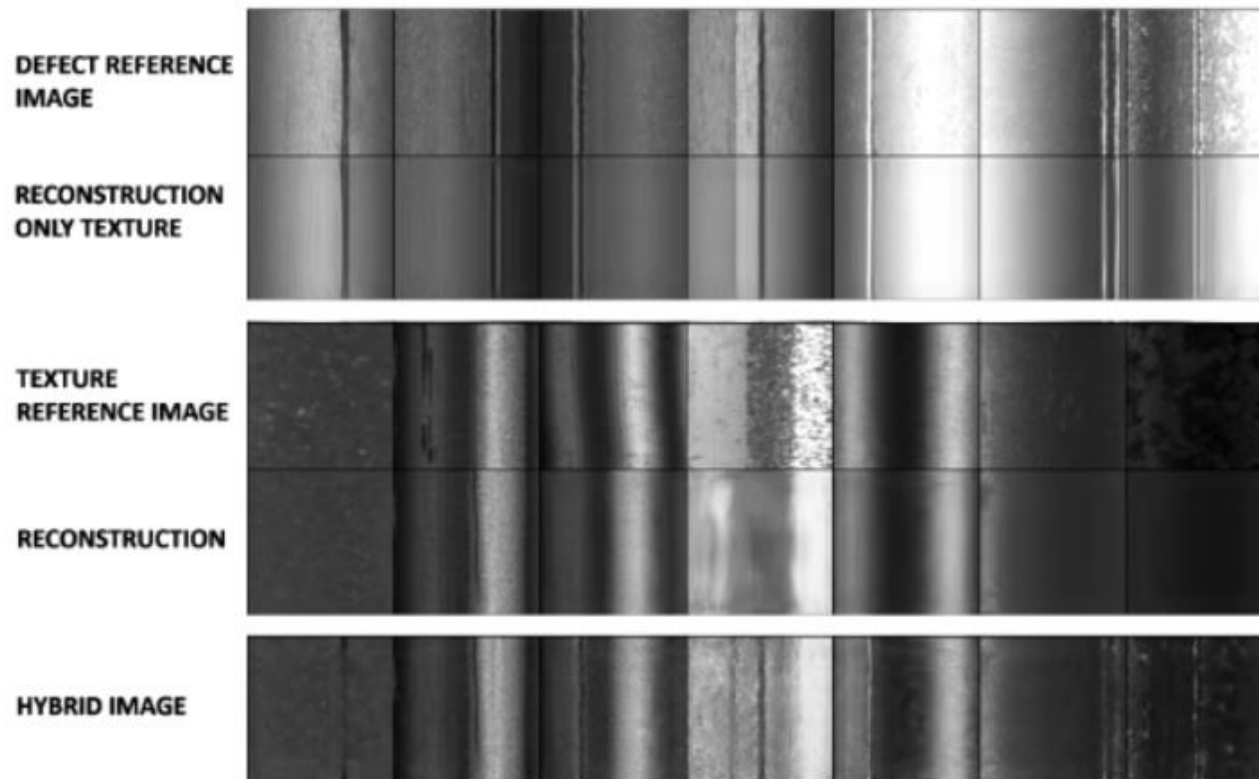


Figure 4.16: Texture reconstruction for the scoring defects. First and third row represents the defect and normal reference images respectively. The second and the fourth row reports the texture reconstruction for the defect and no-defect reference image respectively. The last row instead illustrates the images obtained by swapping the texture code of the defective image with the normal reference image.